Determination of Orbital Elements of 1991 Yuliya PM5 via the Method of Gauss

Team 2 - *Alto*tude: J. Casas, P. Li, A. Zhuang

Etscorn Observatory: (719)
34°04’21.46” N 106°54’51.80” W
Elevation: 1429m
Date: July 21st, 2018

Abstract

Near-Earth asteroids, whose orbits periodically come into Earth’s proximity, have been a source of hazard since the birth of this planet. Determining the orbital elements of these asteroids allows us to track their positions in order to prevent any potential impact. In the following project, we determined the set of orbital elements for 1991 Yuliya PM5, a near-Earth asteroid. Our team collected data on 1991 PM5 over the course of 5 weeks, after which we performed astrometry on our data to calculate the position of the asteroid, photometry to determine its apparent magnitude, and the Method of Gauss to characterize the orbit of the asteroid with calculated orbital elements. We were able to successfully perform these tasks and converge onto many similar sets of orbital elements. After data analysis, we produced a final set of orbital elements for 1991 PM5 that is able to be supported by much evidence.

Introduction

The purpose of this research is to calculate the orbital elements of 1991 PM5, which helps to keep track of the position of the asteroid and prevent any possible future hazardous event. We will also calculate the positions and magnitude of the asteroid to submit to the Minor Planet Center database. To achieve this goal, our team will take images of the asteroid for 5 nights with equal time interval and calculate the position of the asteroid, which will be input into the method of Gauss to generate the orbital elements of the asteroid.

Materials and Methods

The Etscorn Observatory houses the C-14 telescope, which we use to collect our data. The telescope has a 355.5 mm aperture and a 3911 mm focal length, coupled with a 1024 x 1024 pixel array SBIG STL-1001E CCD Chip. Our team also use NASA Jet Propulsion Laboratory Horizons' database to predict the location of 1991 PM5 in order to take images, and TheSkyX to visualize the field of stars when taking these photos and collecting data on stars during data analysis. We use CCDSoft to reduce our images to filter out most of the noise, and Python 3.6.5 to code all of our data processing programs.

Observations

For our observations, we initially planned to image asteroid 1991 PM5 at Etscorn Observatory with the Visual filter with 90.00 second exposures in the raw format, .FIT, without any calibration or auto-reduction. We would later reduce the images with bias, dark, and flat-field frames. After our first observation, we changed our observing strategy because our asteroid appeared to be extremely faint in reduced images. This resulted in the decision to use the Clear filter with an exposure time of 120 seconds. This decision was necessary to assure that our astrometry and photometry could be performed with minimal error.

Calculation Method

The Method of Gauss is computation of orbital elements, done by iteratively calculating position and velocity vectors of the asteroid at a central observation out of three until these vectors' values converge. These values allow one to generate the orbital elements of the asteroid, and different combinations of three can be done if one has more than three sets of data.

Before performing the Method of Gauss, we calculate the right ascensions (RAs) and Declinations (Decs) of the asteroid by performing astrometry on our images. This data, along with the time of each observation and the Earth-to-Sun vectors from JPL Horizons, are our inputs into the Method of Gauss. For our first iteration of the Method of Gauss, we estimate the magnitude of the central observation's position vector with the Scalar Equation of Lagrange, and calculate the central position and velocity vector from a truncated second-order polynomial. Then, using each past value, we iterate using either two

fourth-degree Taylor series, two third-degree Taylor series, or two closed-form functions to keep obtaining better values for position and velocity of the central observation, correcting for light-travel time during each iteration and exiting the iteration once the vector values converge to a set tolerance value. We use the fourth-degree Taylor series for our calculations. The position and velocity vectors allow us to calculate the six orbital elements given a specific epoch, which is July 22, 2018 6:00 UTC in our calculation. This only affects the Mean Anomaly (M), which we will always present as precessed to July 22, 2018 6:00 UTC in this paper.

Since we have five sets of data, we keep the first and last observations, to maximize the range of time of our data, and rotate through the three middle observations to perform the Method of Gauss. Three sets of orbital elements can be calculated from the data we collected.

Additional Procedures

In addition to the Method of Gauss, we also use Differential Correction and Monte Carlo Error Propagation.

Differential Correction is used to correct the orbital elements by minimizing the difference in observed and calculated position and velocity vectors.

Monte Carlo Error Propagation is used to determine the uncertainty of each orbital element by varying our RAs and Decs, running a large amount of these variations through the Method of Gauss, and calculating the standard deviation of the resulting orbital elements. We can then compare these values to the JPL's and MPC's to determine whether our data is within the error bar.

We were also able to roughly visualize the orbit of 1991 PM5 in the solar system.

Data and Analysis

Data Collection

Our team was able to capture data from four observations, with three of those observations being usable for the Method of Gauss. We then acquired more data from Team 11, which observes the same asteroid as us, to complete a set of five observations.

Observation Date/Time	Observing Conditions	Filter	Exposure Time (s)	Number of Images
06/20/18 7:00 - 9:00 UTC	No clouds, clear sky	Visual	90.00	3 sets of 5 frames
06/24/18 3:00 - 5:00 UTC	Sparse clouds	Clear	90.00 / 120.00	3 sets of 5 frames
07/03/18 7:00 - 9:00 UTC	Very cloudy	Clear	120.00	1 set of 5 frames
07/08/18 3:00 - 5:00 UTC	No clouds, clear sky	Clear	120.00	3 sets of 5 frames
07/19/18 5:00 - 7:00 UTC	Sparse clouds	Clear	120.00	2 sets of 5 frames

At this point, we discard our data from June 20, 2018, as the asteroid is hardly visible in the images.

Data Reduction

The raw images taken by the telescope are not immediately useful because the CCD chip not only collected the light from the astronomical objects we are looking for, but also signal from the surrounding electronics and heat sources. It is also highly possible that the telescope has dust on top of the lens, which will appear in the image. To reduce this “noise”, we take three types of calibration images—dark frames, bias frames, and flat-field frames. They reveal the systemic noise of the telescope and the chip. We use CCDSoft to subtract the bias and dark from the raw images and divide away the flat field. Since small positional difference from image-to-image exists, we also need to align our images so the same objects stay in the same position.The reduced and aligned images will be then used for astrometry and photometry.

Centroiding

In order to calculate the right ascension and declination of the asteroid (astrometry), the asteroid's centroid in the images needs to be calculated. We first roughly estimate the center coordinates and dimensions of the asteroid by visual examination, then calculate a weighted mean position of the pixel counts within the given region, which is centroid of the asteroid. The error of the centroid can then be calculated using the equation for standard deviation.

Astrometry

Given the x and y position of the asteroid in the images taken, we can determine the right ascension and declination through the process of Least Square Plane Reduction (LSPR). Twelve stars near the position of asteroid are selected and their centroids calculated. The right ascensions and declinations of the 12 stars are known from a selected star catalog (for us, UCAC3), which can be used to calculate six constants that relate the x and y positions to RA and Dec. The asteroid's RA and Dec can be calculated using these six constants. The error of LSPR astrometry is determined by how far the RAs and Decs of the stars calculated using the six constants are to the actual RAs and Decs from the catalog.

Date/Time	Asteroid's Right Ascension	Asteroid's Declination
06/24/18 3:00 - 5:00 UTC	16h 53m 11.27s 16h 53m 10.71s	+18° 54' 18.9'' +18° 53' 4.4''
07/03/18 7:00 - 9:00 UTC	16h 53m 48.33s 16h 53m 48.31s	+13° 18' 39.6'' +13° 18' 24.7''
07/08/18 3:00 - 5:00 UTC	16h 55m 29.617s 16h 55m 30.241s	+09° 52' 7.3'' +09° 50' 40.3''
07/19/18 5:00 - 7:00 UTC	17h 3m 22.355s 17h 3m 24.241s	+01° 13' 45.5'' +01° 11' 55.8''

Photometry

The apparent magnitude of an astronomical object can be calculated through the equation:

$$Apparent\ Magnitude\ = Instrumental\ Magnitude\ +\ constant$$

Where $Instrumental\ Magnitude = \ -2.5 \times log_{10}(signal)$

Given a centroid position and the radius of the asteroid, we can calculate the signal and instrumental magnitude of the asteroid. In order to get the apparent magnitude, we need to determine the constant. Six reference stars with various magnitudes are chosen and their signal calculated. We plot the base-10 logarithm of the signals of the reference stars against their known apparent magnitude to get a best-fit line for the data. The apparent magnitude of the asteroid can then be calculated using the linear model. The uncertainty of photometry can be determined through the signal-to-noise (SNR) values of the asteroid, which is calculated using the signal value and several other instrumental constants.

Date/Time	Average Sky Brightness (ADU/pixel)	Apparent Magnitude	Signal-to-Noise Ratio (SNR)
06/24/18 3:00 - 5:00 UTC	1080.1402 1144.0579	17.0 17.1	22.6644 24.1310
07/03/18 7:00 - 9:00 UTC	1078.9817 1356.9940	16.6 16.8	20.0628 11.2587
07/08/18 3:00 - 5:00 UTC	524.9746376811594 358.6933962264151	16.8 16.9	31.4838 35.9541
07/19/18 5:00 - 7:00 UTC	582.2424242424242 353.1363636363636	17.2 16.9	18.1119 36.0280

Due to the low SNR values as well as the very cloudy conditions causing our asteroid to look streaked in our images, we did not move forward with data analysis on our observations from July 3, 2018.

Assessing the Validity of Raw Data

The error from centroiding, LSPR astrometry, and photometry each give us different insights of the range of acceptable results from our raw data and calculations. Usually the error from astrometry and photometry is within 1 arcsec and 0.05 magnitude, respectively. The SNR values calculated from photometry tells us the amount of noise present in our images. After each calculation, we always look up data from credible databases such as JPL Horizons to verify the validity of our raw data and calculation processes.

Input Data for the Method of Gauss

Date/Time	Asteroid's Right Ascension	Asteroid's Declination	Sun Vector * (AU)	
**06/21/18 07:47:27.00 UTC	16h 53m 32.13s	+20° 20' 54.2''	x	$6.060773031529278 \cdot 10^{-3}$
			y	$9.324028920457019 \cdot 10^{-1}$
			z	$4.041625952374700 \cdot 10^{-1}$
06/24/18 04:51:13.39 UTC	16h 53m 10.71s	+18° 53' 4.4''	x	$-4.259608920306333 \cdot 10^{-2}$
			y	$9.317362919229669 \cdot 10^{-1}$
			z	$4.038763149316724 \cdot 10^{-1}$
07/08/18 04:17:16.00 UTC	16h 55m 30.241s	+09° 50' 40.3''	x	$-2.755610982260392 \cdot 10^{-1}$
			y	$8.979244509017437 \cdot 10^{-1}$
			z	$3.892129128647434 \cdot 10^{-1}$
**07/17/18 05:26:11.00 UTC	17h 01m 30.52s	+02° 49' 45.8''	x	$-4.191969378578619 \cdot 10^{-1}$
			y	$8.495494152817795 \cdot 10^{-1}$
			z	$3.682464162695799 \cdot 10^{-1}$
07/19/18 05:23:54.00 UTC	17h 3m 22.36s	+01° 13' 45.5''	x	$-4.497179470127340 \cdot 10^{-1}$
			y	$8.361688570133541 \cdot 10^{-1}$
			z	$3.624468597378236 \cdot 10^{-1}$

* Generated from JPL Horizons

** Data obtained from Team 11

Team Member	OE	Observations 1, 2, 5	Observations 1, 3, 5	Observations 1, 4, 5
Jorge Casas	a	1.69369 AU	1.72229 AU	1.74618 AU
	e	0.24702	0.25599	0.26354
	i	14.14603 °	14.44912 °	14.67475 °
	Ω	132.91056 °	132.58303 °	132.34340 °
	ω	140.09461 °	140.61902 °	140.99851 °
	M	8.91942 °	8.50121 °	8.1858489 °
Pearl Li	a	1.69294 AU	1.72164 AU	1.74568AU
	e	0.24678	0.25579	0.26338
	i	14.13819 °	14.44256°	14.66971 °
	Ω	132.91918 °	132.59000°	132.34864 °
	ω	140.08034 °	140.60893°	140.99170 °
	M	8.93081 °	8.50962°	8.19170 °
Ashley Zhuang	a	1.69294 AU	1.72164 AU	1.74567 AU
	e	0.24678	0.25579	0.26338
	i	14.13819 °	14.44256 °	14.66971 °
	Ω	132.91918 °	132.59000 °	132.34864 °
	ω	140.08034 °	140.60893 °	140.99170 °
	M	8.93081 °	8.50962 °	8.19170 °

Orbital Elements

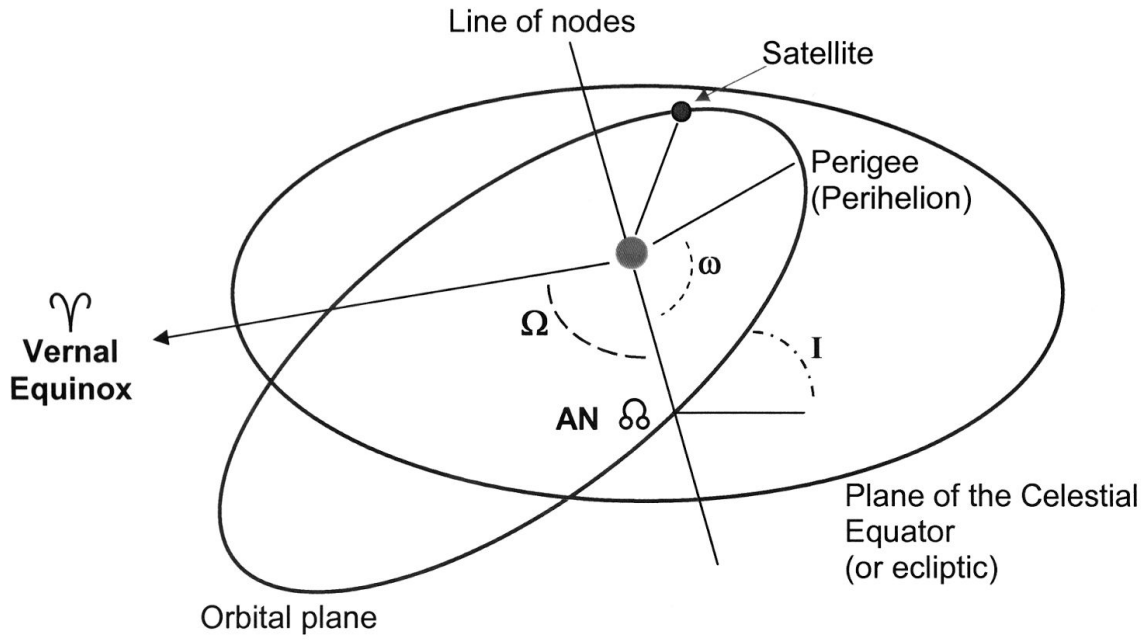

Mean distance (a) is the length of semi-major axis of the elliptical orbit in astronomical units. Eccentricity (e) is the ratio of the semi-major axis and the distance from the center to the two focis. It measures the degree of elongation of the elliptical orbit. Inclination (i) is the angle in degrees between the asteroid's orbit plane and the ecliptic plane. Longitude of ascending node (Ω) is the angle in degrees between the vernal equinox and the line of nodes where the ecliptic plane and the asteroid's orbital plane intersect. Argument of perihelion (ω) is the angle in degrees from the ascending node to the perihelion, where the asteroid is closest to the Sun. Mean anomaly (M) defines the position of the asteroid along its orbit at a reference epoch.

Differential Correction

In order to improve upon our orbital elements, we perform differential correction on our input data. The goal of this process is to slightly adjust our position and velocity vectors of a central observation in order to minimize the difference between the observed right ascensions and declinations and those calculated from our orbital elements.

To quantify how well our orbital elements fit our observed data, we calculated the root-mean-square (RMS) of our right ascensions and declinations with the following equation:

$$RMS = \sqrt{\frac{\sum(O-C)^2}{n-6}},$$

where O is observed value, C is calculated value, and n is twice the number of usable observations. Ideally, RMS would be zero. Below is a table of our RMS values prior to differential correction:

Team Member	Combination of Obs.	RMS from Method of Gauss
Jorge Casas	1, 2, 5	$1.637 \cdot 10^{-4}$
	1, 3, 5	$1.927 \cdot 10^{-5}$
	1, 4, 5	$1.501 \cdot 10^{-4}$
Pearl Li	1, 2, 5	$1.649 \cdot 10^{-4}$
	1, 3, 5	$1.835 \cdot 10^{-5}$
	1, 4, 5	$1.506 \cdot 10^{-4}$
Ashley Zhuang	1, 2, 5	$1.649 \cdot 10^{-4}$
	1, 3, 5	$1.834 \cdot 10^{-5}$
	1, 4, 5	$1.506 \cdot 10^{-4}$

Since Zhuang's position and velocity vectors from the Method of Gauss for observation's 1, 3, and 5 yielded the smallest RMS value, they are the best fit for our data. Thus, we use these vectors to perform differential correction to further improve the best RMS value. After correction, the RMS is decreased to $5.497 \cdot 10^{-6}$ and the orbital elements are improved to the following values:

a: 1.71870 AU
e: 0.25485
i: 14.41425°
Ω: 132.62049°
ω: 140.56109°
M: 8.54944°

Monte Carlo

To analyze the error in our orbital elements, we use the Monte Carlo method of error propagation. The uncertainty of the right ascensions and declinations calculated from the Least Squares Plate Reduction measures how well our calculation of right ascensions and declinations of certain stars in our images matched their known right ascensions and declinations from the UCAC3 star catalog. The following is a table of these uncertainties for the images we used in the Method of Gauss

Date/Time	RA Uncertainty (arcseconds)	Dec. Uncertainty (arcseconds)
**06/21/18 07:47:27.00 UTC	5.3	0.6
06/24/18 04:51:13.39 UTC	0.4	0.5
07/08/18 04:17:16.00 UTC	0.6	0.6
**07/17/18 05:26:11.00 UTC	5.5	0.6
07/19/18 05:23:54.00 UTC	10.0	6.0

** All data from these dates are Team 11's data

We generated a Gaussian distribution of 500,000 RAs and Decs centered at our calculated RAs and Decs with standard deviations of the uncertainties in the table above. By running these values through the Method of Gauss, we were able to obtain 500,000 sets of orbital elements. The graphs of the Gaussian distribution of the six orbital elements shown below indicate the amount of change resulted from slight deviations of RAs and Decs. We use the observations 1, 3, and 5, which produces the lowest RMS values, to perform the Monte Carlo method. The following graphs show the resulting distribution of each orbital element:

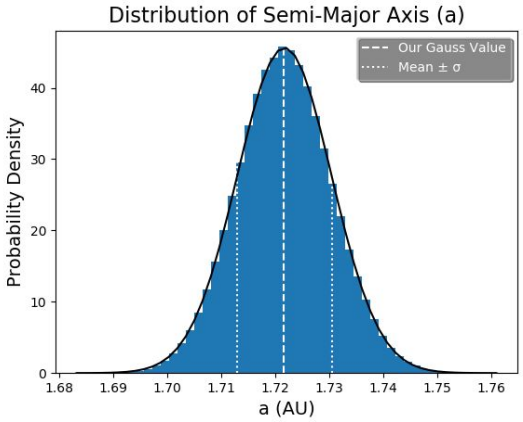

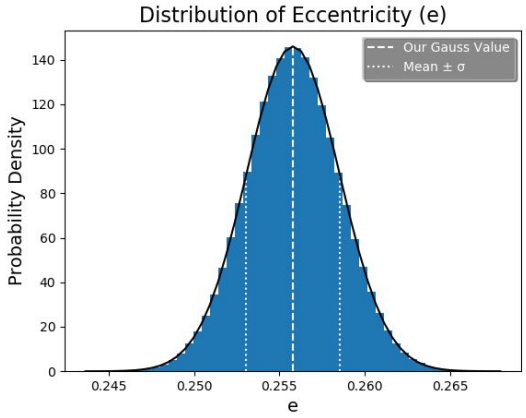

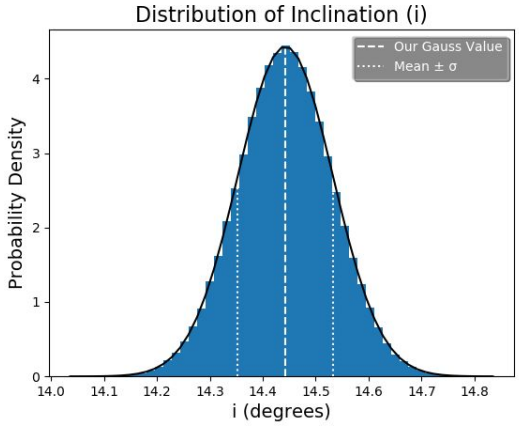

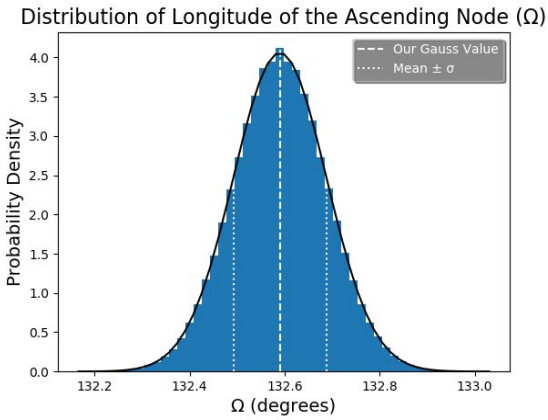

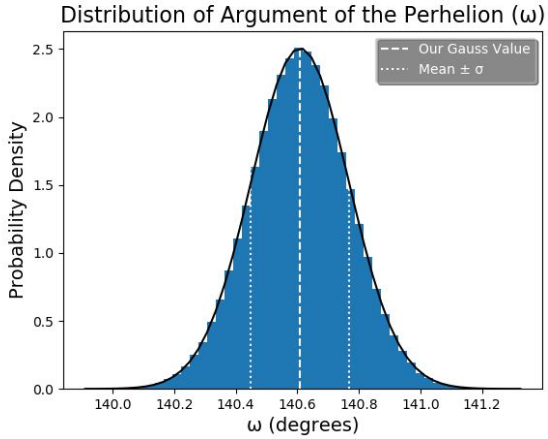

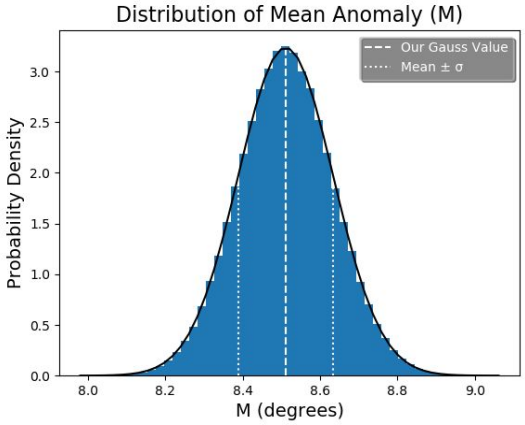

From the distribution graphs, we obtain the arithmetic mean, median, and standard deviation of each orbital element. We compare the centers of these graphs to our best values (lowest RMS) from the Method of Gauss before differential correction:

Orbital Element	Our Value	Mean	Median	Standard Deviation
a (AU)	1.72164	1.72171	1.72165	0.009
e	0.25579	0.25580	0.25579	0.009
i (°)	14.44256	14.44269	14.44264	0.090
Ω (°)	132.59000	132.59000	132.58986	0.100
ω (°)	140.60893	140.60872	140.60930	0.200
M (°)	8.50962	8.51088	8.51027	0.100

Since our values are very close to the centers of these normal distributions, it is reasonable to assume that the uncertainties in the orbital elements is the standard deviation of the Gaussian distributions. Differential correction would not affect these uncertainties because the process attempts to match our calculated values to the original RAs and Decs that were observed, and Monte Carlo gives us how the error in these RAs and Decs propagate to error in orbital elements. Thus, our final orbital elements, obtained from differential correction, with uncertainty are as follows:

$a = 1.719 \text{ AU} \pm 0.009 \text{ AU}$
$e = 0.255 \pm 0.003$
$i = 14.41° \pm 0.09°$
$\omega = 132.6° \pm 0.1°$
$\Omega = 140.6° \pm 0.2°$
$M = 8.5° \pm 0.1°$

	Position generated from our Calculated Orbital Elements		Team 11's measured Asteroid position	
Observation Time(UTC)	**RA**	**Declination**	**RA**	**Declination**
06/21/18 07:47:27	16h 53m 32.29s	20° 20' 54.8''	16h 53m 32.13s	20° 20' 54.2"
06/25/18 04:03:35	16h 53m 7.16s	18° 21' 30.6''	16h 53m 6.79s	18° 21' 29.7"
07/09/18 06:05:29	16h 56m 0.46s	09° 2' 35.6''	16h 56m 0.48s	09° 02' 35.6"
07/17/18 05:26:11	17h 1m 30.50s	02° 49' 45.6''	17h 01m 30.52s	02° 49' 45.8"

The above table compares the observed right ascension and declination of the other team's data to those calculated from our orbital elements. The root-mean-square value for the right ascensions and declinations is $2.112 \cdot 10^{-5}$ (see Differential Correction for RMS formula). This indicates that our orbital elements correctly predict the other team's data with a small margin of error, further validating our orbital element computation.

Comparison to JPL and MPC

To further assess the validity of our orbital elements, we compare our values to the most recently generated orbital elements from NASA Jet Propulsion Laboratory (JPL) Horizons and Minor Planet Center (MPC):

Orbital Element	Our Value	JPL Horizons Value	MPC Value
a (AU)	1.719 ± 0.009	1.719501170685847	1.7196424
e	0.255 ± 0.003	0.2553809371785112	0.2551449
i (°)	14.41 ± 0.09	14.42810965774444	14.42643
Ω (°)	132.6 ± 0.1	132.6415454581062	132.62962
ω (°)	140.6 ± 0.2	140.565110252241	140.55084
M (°)	8.5 ± 0.1	8.572234328	8.42634622

All of the JPL and MPC values are within the uncertainty of our orbital elements.

Classification and Brief History of 1991 Yuliya PM5

Since the calculated semi-major axis of Yuliya is greater than 1.0 AU, it falls under either the Amor or Apollo groups of asteroids. To further specify, we need to calculate the r_{min} (distance to Sun at perihelion) using the following equation:

$$r_{min} = a(1 - e) = 1.2807AU$$

Yuliya is an the Amor asteroid because its r_{min} values is greater than 1.017 AU but smaller than 1.3 AU. Amor asteroids have the following characteristics: they have an orbit outside the Earth's orbit, periodically come close to Earth, and never cross the orbit of Earth.

15745 Yuliya 1991 PM5 was discovered back in August 3, 1991 at La Silla Observatory in Chile by Belgium astronomer Eric Walter Elst, who is credited with the discovery of a total of 3,866 minor planets between 1986 and 2009.

1991 PM5 was named after Yuliya Germanova, who served as a translator at the 2013 "First International Conference on the Chelyabinsk/Chebarkul Meteor/Meteorite."

Its closest near-miss Earth distance is 8,794,642 kilometers, about 0.0588 AU on August 25, 2097.

Conclusion

From our usage of the Method of Gauss, differential correction, and Monte Carlo, we are able to determine the orbital elements of 1991 Yuliya PM5: a = 1.719 AU ± 0.009 AU, e = 0.255 ± 0.003, i = 14.41° ± 0.09°, ω = 132.6° ± 0.1°, Ω = 140.6° ± 0.2°, M = 8.5° ± 0.1°. We are able to validate our findings by finding the root-mean-square values, which compares the right ascensions and declinations calculated from the orbital elements to the observed values, which yields a number of 10^{-6} order. Additionally, our orbital elements generate similar values to the observed right ascensions and declinations of the other team's data, yielding a root-mean-square value of 10^{-5} order. Our data is further supported by the JPL and MPC calculations of Yuliya's orbital elements, which all fall within our margin of uncertainty.

We are also able to categorize Yuliya as an Amor asteroid using the calculated semi-major axis and eccentricity. We can model the positions and vectors of Yuliya at any given time using the orbital elements, which provides a means to track the asteroid's future evolution and possible influence on Earth.

Sources of unavoidable errors includes instrumental errors of the telescope and CCD chip, centroiding error resulting from human error in visual examination, LSPR error from the discrepancy between calculated and known right ascension and declinations of the reference stars, and photometry error resulted from extrapolation and the noise collected by the CCD chip. The Earth-to-Sun vectors we use in the Method of Gauss is from JPL horizons, which is a source of bias.

Instead of using the JPL Earth-to-Sun vectors without any verification, we should calculate the Earth-to-Sun vectors ourselves to have unbiased results. We should also try to expand the Method of Gauss f and g Taylor series into higher degrees to get more accurate results. The Method of Gauss is also only a preliminary way to converge to a set of orbital elements. If time allows, we should also use the method of Laplace to confirm our results.

When replicating this project, try to observe with equal time intervals, which may allow the Method of Gauss to produce more accurate results. Organization of different categories of data including images, x and y position, right ascension and declinations, reference star informations, photometry will make the calculation process cleaner and easier. Referencing multiple credible databases is a good way to minimize bias as you check intermediate values.

Appendices

MPC Report

COD 719
CON A. W. Rengstorf
CON [adamwr@purduecal.edu]
OBS J. Casas, P. Li, A. Zhuang
MEA J. Casas, P. Li, A. Zhuang
TEL 0.3556m f/11 Schmidt Cassegrain + CCD
NET UCAC3
BND R
NUM 6
ACK Team 2 - 15745 Yuliya(1991 PM5)

15745	C2018 06 24.16299 16 53 11.27 +18 54 18.9	17.0 R	719
15745	C2018 06 24.20224 16 53 10.71 +18 53 04.4	17.1 R	719
15745	C2018 07 08.14550 16 55 29.62 +09 52 07.3	16.8 R	719
15745	C2018 07 08.17866 16 55 30.24 +09 50 40.3	16.9 R	719
15745	C2018 07 19.22493 17 03 22.36 +01 13 45.3	17.2 R	719
15745	C2018 07 19.30128 17 03 24.24 +01 11 55.8	16.9 R	719

Cloud Night Experiment

Data collection strategy and methodology:

The cloudy nights experiment is divided into three separate nights of data collection: dark frames with increasing exposure time, dark frames with decreasing temperature, and bias frames with decreasing temperature. During the first night, 7 sets of dark frame images are taken at constant CCD temperature. Starting with an exposure time of 5 second, each set doubles the exposure time of the previous set until pixel counts exceeds 1e4 ADU. At the second and third cloudy night, 3 sets of dark frame and 19 sets of bias frame images are taken with respect to the changing temperature of the CCD chip.

Assumptions:

Given constant CCD chip temperature, longer exposure time allows more photons to be collected. Assuming that photons approaches the chip at a constant rate, we hypothesize a linear relationship between the dark current signal collected per pixel and exposure time. Given constant exposure time and assuming that a warmer CCD chip has more dark current, the relationship between chip temperature and the rate of dark signals collected is also hypothesized to be linear. Bias frame signal is the digitization noise of the CCD chip itself, which we assume will be constant regardless of the chip temperature. The hypothesis is that bias frames do not depend on temperature.

Results:

Cloudy Night 1:

The best fit line for the relationship between dark current signal in electrons and exposure time is:

$$De^- = 61.8702t - 646.9914$$
$$De^- : \textit{Dark current signal in electrons/pixel}$$
$$t : \textit{exposure time in seconds}$$

With correlation coefficient $r = 0.9968766483$.

However, through visual examination of the best fit line and the scatter plot, there appears to be a parabolic pattern associated with the data. A quadratic regression is performed and the best fit 2-degree polynomial for the relationship along with the uncertainty of the coefficients are calculated as below:

$$De^- = (0.0578 \pm 0.0038)t^2 + (43.5034 \pm 1.2555)t - (108.8007 \pm 57.374)$$

With coefficient of determination $r^2 = 0.999946024$.

The regression model illustrates a strong parabolic relationship between dark current signal and exposure time.

Cloudy Night 2:

Arrhenius law describes a exponential relationship between the reaction rates and inverse of temperature. Assuming that the dark frame images agree with Arrhenius law, the best fit linear relationship between dark current rate per pixel and inverse of chip temperature is:

$$eq1 : ln(De^-/s) = -1.8421 \times 10^{-19}/kT + 57.9249$$
$$De^-/s : \textit{Dark current signal in electrons per pixel/total exposure time}(120s)$$
$$T : \textit{chip temperature in Kelvin}$$
$$k : \textit{Boltzmann's constant}$$

Using Arrhenius law, Ralf Widenhorn expresses the exponential relationship between dark count rates and temperature as:

$$eq2 : De^-/s = De_0{}^-/s \times e^{(-\triangle E/kT)}$$

Taking the natural log of both sides, we get:

$$ln(De^-/s) = -\triangle E/kT + ln(De_0{}^-/s)$$

Comparing eq. 1 and eq. 2, we get the average activation energy and prefactor of the CCD chip:

$$\textit{Activation energy } (\triangle E) = = -1.8421 \times 10^{-19}$$
$$Prefactor(De_0{}^-) = e^{57.9249} = 1.4337 \times 10^{25}$$

Cloudy Night 3:

A distinct exponential relationship between bia frame signals and temperature can be deduced from visual examination of the scatter plot. The best fit exponential model calculated is:

$$Be^{-} = 3.3127e^{0.1830T-0.3653} + 2009.9212$$

$$Be^{-} : Bias\ signal\ in\ electrons/pixel$$

$$T : chip\ temperature\ in\ Kelvin$$

Plots:

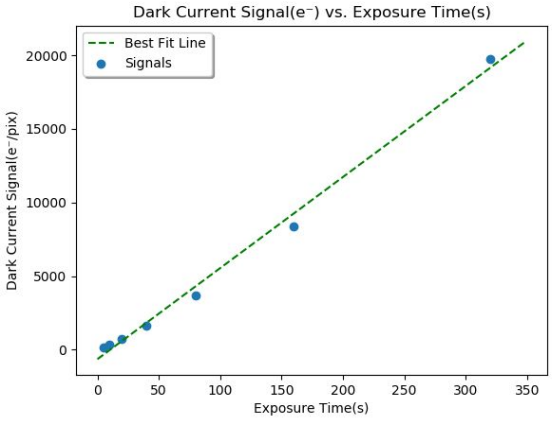

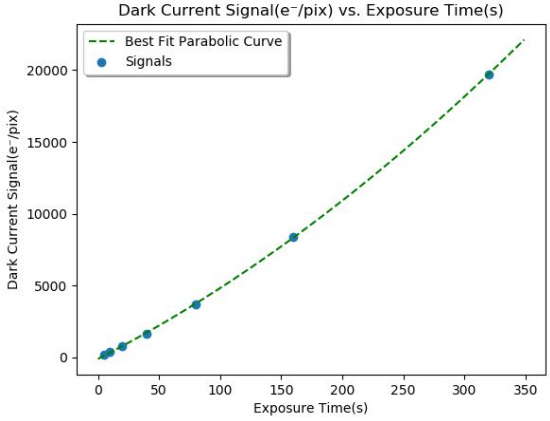

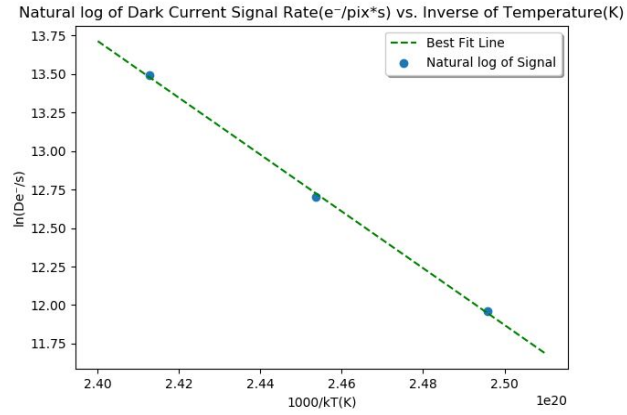

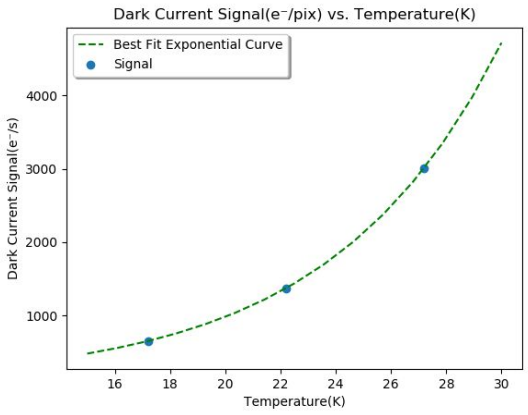

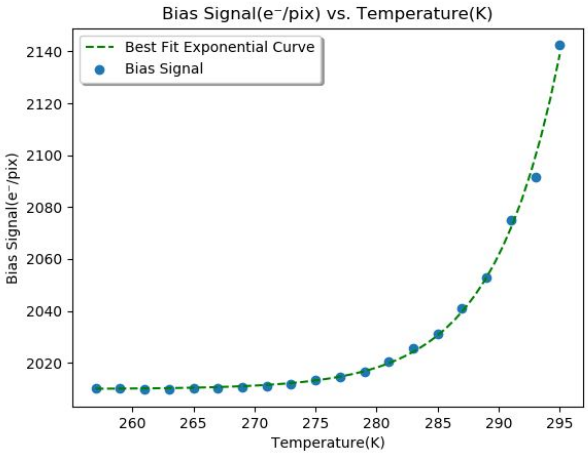

Data analysis:

The uncertainty of the signal is the variation of a pixel from one image to another. Using the standard deviation for two data points:

$$\sigma = \frac{|x_2 - x_1|}{\sqrt{2}}$$

The average uncertainty of signal can be calculated through comparing pairs of images. By comparing images 1 and 2, 2 and 3, 3 and 4, and 4 and 5 of the first set of Dark current vs. exposure time, we can calculate an average uncertainty of the set. Similar calculations are performed for all other data sets of the three nights.

Interestingly, the uncertainty from experiment to experiment exhibit different relationship with the independent variables.

As illustrated by the graphs below, the relationship between signal uncertainty of dark frame images and exposure time is exponential while the relationship between the same uncertainty and temperature is linear.

Uncertainty of bias frame images and temperature exhibits a negative exponential relationships where the uncertainty gradually flattens out as temperature increases.

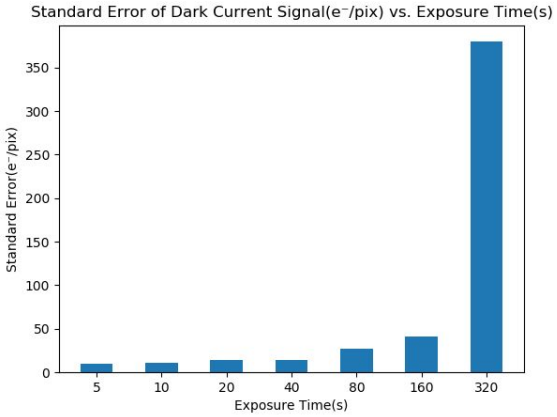

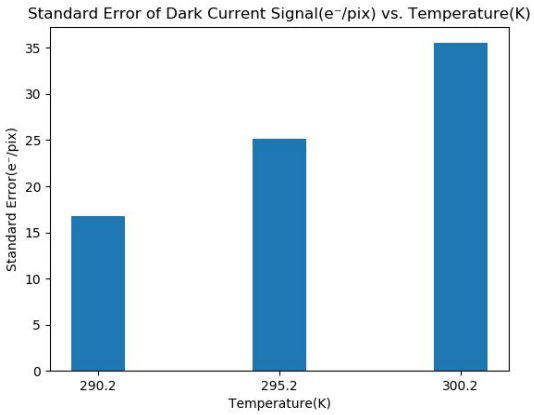

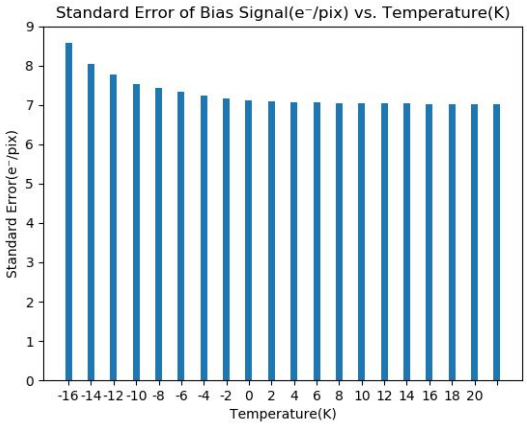

Discussion and conclusion:

None of the initial hypotheses are supported by the data collected as none of the relationships is linear. Dark current signal and exposure time exhibits a parabolic relationship while that between dark current signal rate and temperature is exponential. Finally, bias frame signal and temperature has an exponential relationship. Sources of discrepancy might be undersampling and uneven temperature interval during the data collecting process.

Work cited

Widen, R. et al, "Temperature dependence of dark current in a CCD," Proc. SPIE 4669, 193-201(2002).

Koblick, D (2013, Dec 12). *Convert Keplerian Orbital Elements to a State Vector* [Infographic]. Retried from https://ww2.mathworks.cn/matlabcentral/fileexchange/35455-convert-keplerian-orbital-elements-to-a-state-vector?focused=3804003&tab=function

Schmadel, L(2012-2014). *Dictionary of Minor Planet Names: Addendum to 6th Edition,* Retrieved from https://books.google.com/books?id=dzBsCQAAQBAJ&pg=PA114&lpg=PA114&dq=Yuliya+Germanova&source=bl&ots=2lyGNvpL_l&sig=Kfr1xR6JX2mmFmfW8KLcMm_H6ZU&hl=en&sa=X&ved=0ahUKEwjw7cbl-bHcAhWCCTQIHQ8qCsEQ6AEIUTAJ#v=onepage&q=Yuliya%20Germanova&f=false